LETTERS
PUBLISHED ONLINE: 17 MAY 2009 | DOI: 10.1038/NGEO521
nature geoscience

In situ detection of biological particles in cloud ice-crystals

Kerri A. Pratt[1], Paul J. DeMott[2]*, Jeffrey R. French[3], Zhien Wang[3], Douglas L. Westphal[4], Andrew J. Heymsfield[5], Cynthia H. Twohy[6], Anthony J. Prenni[2] and Kimberly A. Prather[1,7]*

The impact of aerosol particles on the formation and properties of clouds is one of the largest remaining sources of uncertainty in climate change projections[1]. Certain aerosol particles, known as ice nuclei, initiate ice-crystal formation in clouds, thereby affecting precipitation and the global hydrological cycle[2]. Laboratory studies suggest that some mineral dusts and primary biological particles—such as bacteria, pollen and fungi—can act as ice nuclei[3]. Here we use aircraft-aerosol time-of-flight spectrometry to directly measure the chemistry of individual cloud ice-crystal residues (obtained after evaporation of the ice), which were sampled at high altitude over Wyoming. We show that biological particles and mineral dust comprised most of the ice-crystal residues: mineral dust accounted for ~50% of the residues and biological particles for ~33%. Along with concurrent measurements of cloud ice-crystal and ice-nuclei concentrations, these observations suggest that certain biological and dust particles initiated ice formation in the sampled clouds. Finally, we use a global aerosol model to show long-range transport of desert dust, suggesting that biological particles can enhance the impact of desert dust storms on the formation of cloud ice.

Although ice-nucleation-active bacteria have been detected in the clear atmosphere up to 7 km (ref. 4), previous measurements of biological particles in cloud have focused on offline measurement methods following collection of low-altitude liquid-phase bulk cloud water[5,6]. In this study, real-time measurements of ice-nucleating particle concentrations were made in parallel with size-resolved chemical composition measurements of individual ice-particle residues, both concurrent with cloud phase measurements. Following selection of individual cloud particles by a counterflow virtual impactor (CVI), water was evaporated, providing residual particles for real-time, *in situ* mass spectrometric analysis[7]. To detect submicrometre ice-nucleating aerosol particles in real time, residual particles were re-processed within a continuous-flow diffusion chamber (CFDC) simulating the sampled cloud conditions[8]. Simultaneous *in situ* measurements of the size-resolved chemical composition of individual submicrometre residual particles were made using aircraft-aerosol time-of-flight mass spectrometry (A-ATOFMS), providing the first aircraft-based, single-particle, dual-polarity mass spectrometry measurements[9]. Measurements of an orographic wave cloud were made aboard the National Science Foundation/National Center for Atmospheric Research C-130 aircraft over Wyoming (43° N, 107°–108° W) at 7.9–8.3 km above mean sea level (m.s.l.) on 7 November 2007 during the Ice in Clouds Experiment—Layer Clouds (ICE-L).

To characterize the physical properties of the target orographic wave cloud, time series profiles were examined for the following aircraft-based measurements: radar reflectivity, ice-crystal effective diameter and ice-crystal (>50 μm) number concentrations, as well as aerosol residue (0.5–1.2 μm in diameter) and CFDC ice-nuclei number concentrations derived from the CVI residual particles (Fig. 1). At ~21:09 UTC, an ice cloud at −31 °C was entered in a downstream to upstream pass along the wind vector at ~7.9 km m.s.l. Ice-crystals were observed in concentrations of $13.8 \pm 3.7\,l^{-1}$, with average ice-nuclei concentrations of $1.6 \pm 1.3\,l^{-1}$ measured at −31 °C from the CVI residual particles. At ~21:15 UTC, the same cloud was entered at a higher elevation (~8.3 km) and lower temperature (−34 °C) in the opposite direction (downwind–upwind). The CFDC temperature was lowered from −31 to −34 °C to match the cloud temperature at this level. Both ice-crystal and ice-nuclei concentrations (averages of $56.6 \pm 7.5\,l^{-1}$ and $4.7 \pm 2.2\,l^{-1}$, respectively) were higher for this flight leg. The regions of higher radar reflectivity at altitudes below ~8.7 km in both passes suggest the presence of large ice particles through a deep layer, which is supported by effective ice-crystal sizes up to 200 μm. Radar and lidar data indicate that the cloud extended to ~10.3 km in altitude; however, 8.3 km was the maximum aircraft altitude. Ice-crystal dimensions up to 1,500 μm and 1,000 μm were measured in the two respective cloud passes (see Supplementary Fig. S1), suggesting that some ice-crystals settled from higher altitudes; this is supported by the distribution of radar-derived Doppler crystal fallspeeds having a modal value of $0.7\,m\,s^{-1}$ during both cloud passes. In addition, at the highest cloud altitudes, the effective crystal sizes support the presence of smaller crystals in higher number concentrations.

Overall, these results suggest that ice formation was dominated by heterogeneous ice-nucleation processes in the cloud regions sampled, but with significant contributions of particles nucleated at higher altitude and lower temperatures settling into the flight level. Heterogeneous processes are the only viable source for ice formation based on the cloud pass temperatures (−31 to −34 °C) alone[10]. Nevertheless, as indicated, the cloud extended more than 1.5 km above the highest flight level, with consequent temperatures as low as −40 °C that also permit homogeneous freezing nucleation if saturation conditions rise to water saturation

[1]Department of Chemistry and Biochemistry, University of California, San Diego, La Jolla, California 92093, USA, [2]Department of Atmospheric Science, Colorado State University, Fort Collins, Colorado 80523, USA, [3]Department of Atmospheric Science, University of Wyoming, Laramie, Wyoming 82071, USA, [4]Marine Meteorology Division, Naval Research Laboratory, Monterey, California 93943, USA, [5]Mesoscale and Microscale Meteorology Division, National Center for Atmospheric Research, Boulder, Colorado 80305, USA, [6]Department of Oceanic and Atmospheric Sciences, Oregon State University, Corvallis, Oregon 97331, USA, [7]Scripps Institution of Oceanography, University of California, San Diego, La Jolla, California 92093, USA.
*e-mail: pdemott@lamar.colostate.edu; kprather@ucsd.edu.

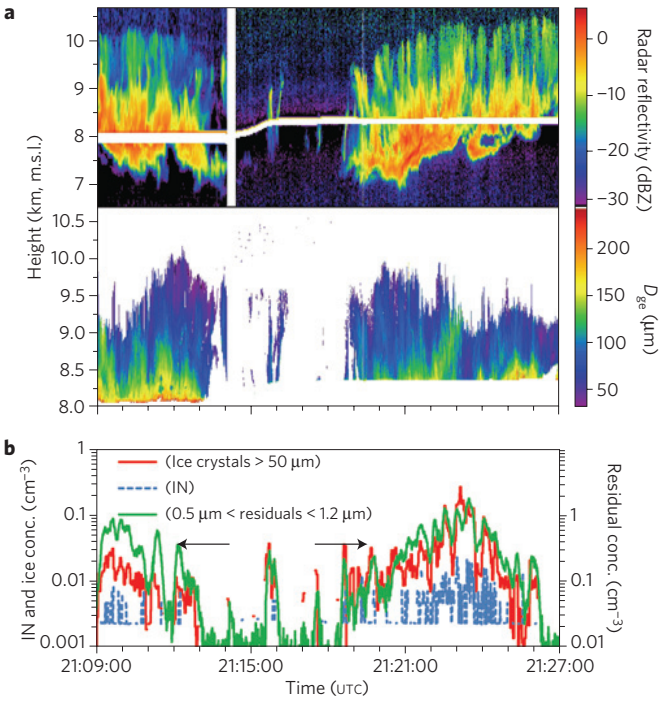

Figure 1 | Ice-cloud microphysical properties. a, Upward- and downward-pointing radar reflectivity with respect to flight time and derived general effective size (D_{ge}) of ice-crystals from combined lidar and radar measurements. **b**, Aerosol (0.5–1.2 μm) and ice-nuclei (IN) number concentrations measured in series with the CVI with respect to flight time. Ice-crystal (>50 μm) number concentrations (2D-C) were measured in parallel to the CVI measurements. All concentrations are 1 Hz data except the aerosol (30 s running mean). Arrows indicate wind direction through cloud.

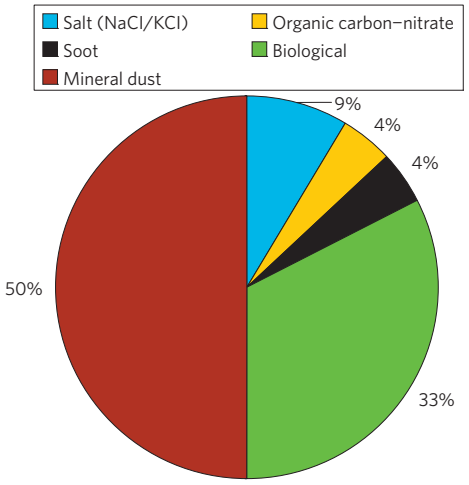

Figure 2 | Chemical composition of ice-crystal residues. Relative contributions of different particle types as measured by the A-ATOFMS for 46 submicrometre (140–700 nm) ice residual particles sampled from 21:09–21:27 UTC. 60 ± 13% of the mineral dust was internally mixed with humic and/or biological material.

in cloud parcels. However, the influence of homogeneous freezing is inferred only for a short period along the cloud pass at ~21:23 UTC when the concentrations of ice-crystals below 30 μm increased sharply (see Supplementary Fig. S1). Although ice-crystal concentrations exceed CFDC ice-nuclei number concentrations by an order of magnitude on average, we believe that lower ice-nuclei concentrations primarily reflect CFDC processing at a temperature warmer than the heterogeneous ice-nucleation temperature of the settled ice-crystals (see Supplementary Information for further mechanistic discussion). We also note that ice-nucleus and ice-crystal concentrations agree best at cloud inflow regions and show poorer agreement deep in the cloud where crystal sedimentation was occurring. Although consideration of ice-nucleation mechanisms alone suggests that ice-crystal residual compositions are representative of heterogeneous ice nuclei and some contribution from particles freezing homogeneously, the concentrations of cloud residual particles were greater than the measured ice-crystal concentrations, indicating extra non-nucleation-related scavenging of particles.

During ICE-L, A-ATOFMS provided *in situ* detection of biological particles[11,12] in real time from the residues of individual cloud droplets and ice-crystals, as discussed in Supplementary Information. As shown in Fig. 2, biological and mineral-dust particles represented most (83 ± 6%) of the ice-crystal residues within the high-altitude ice cloud. 50 ± 12% of the ice residues were found to be mineral dust and 33 ± 10% biological residues. Minor ice-crystal residue particle types included salts (sodium/potassium chloride), organic carbon mixed with nitrate, and soot. The positive- and negative-ion mass spectra of a representative biological ice residual particle are shown in Fig. 3a. This 260 nm biological residue is characterized by calcium, sodium, organic carbon, organic nitrogen and phosphate. More intense ion signals from the inorganic components compared with carbonaceous species result from lower ionization potentials and do not reflect mass fractions. Biological mass spectral signatures can be differentiated from dust on the basis of abundant organic and phosphorus ions, as well as a lack of key dust markers, such as aluminium and silicates. All sampled biological particles contained nearly identical negative-ion mass spectral markers with positive-ion organic markers. The ion signals of the inorganic components, namely sodium, magnesium, potassium and calcium, differed in intensity within the individual particles, suggesting a diversity of biological particle types, including bacteria, fungal spores and/or plant material.

Importantly, the use of dual-polarity mass spectrometry enabled the A-ATOFMS to unambiguously distinguish biological particles from non-biological carbonaceous and inorganic particles, a previous limitation in the detection of biological particles in cloud ice[3]. Previous real-time measurements of ice-nuclei and ice-crystal residues have shown dominant contributions by mineral dust[13,14]. The positive- and negative-ion mass spectra of a representative mineral-dust ice residual particle are shown in Fig. 3b. This 340 nm dust particle, representative of a phyllosilicate clay particle[15], is characterized by intense inorganic markers, including sodium, magnesium, potassium, calcium, iron and aluminosilicates, as well as less intense ion markers of organic nitrogen and phosphate. Most (87 ± 8% by number) of the mineral-dust particles detected in the cloud ice residues were characterized as phyllosilicate clays, such as illite, montmorrillonite and kaolinite[15], which are known ice nuclei[16]. 60 ± 13% of the dust particles contained both organic nitrogen and phosphate, suggesting internal mixing of biological material with the mineral dust, which may have increased the ice-nucleation efficiency of the dust. Less than half (30 ± 17%) of the sampled dust particles contained nitrate and/or sulphate, and no ammonium was detected on any dust particles, similar to previously measured mineral-dust ice residues[14]. This suggests lofting to high altitudes near the source of the dust storm, followed by transport in the mid and upper troposphere, with very low interactions of the dust with pollutants during transport. As recent laboratory studies have shown decreased ice-nucleation efficiencies for mineral dust coated by nitrate, sulphate and organics[17], it is possible that the coated mineral dust, as well as the minor salt and organic carbon particle types observed, froze homogeneously or were

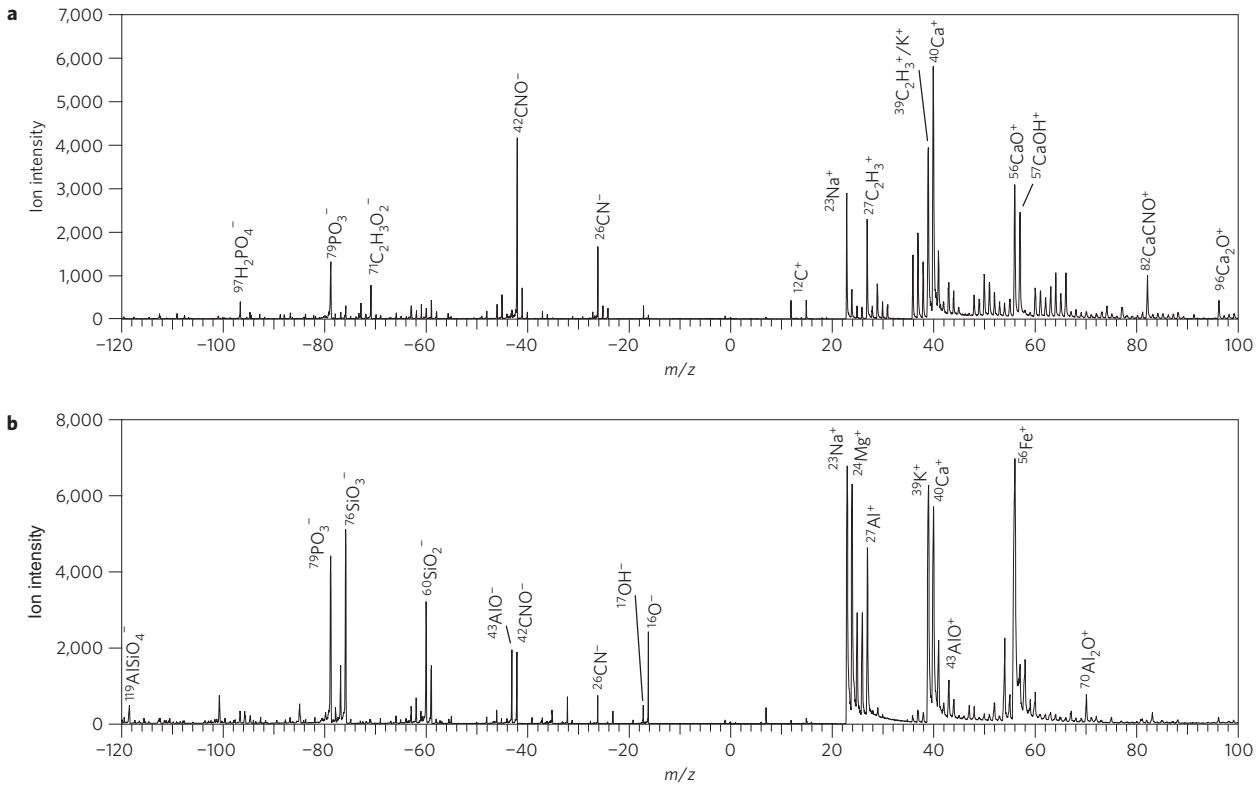

Figure 3 | Representative chemical composition of biological and dust particles. Positive- and negative-ion mass spectra of representative individual biological (**a**) and mineral-dust (**b**) CVI ice residual particles.

scavenged by falling ice-crystals within the deep cloud. As discussed in Supplementary Information, cloud ice-residue mineral-dust and biological-particle number fractions were each enhanced by a factor of ~3 compared with clear air, suggesting preferential nucleation and/or scavenging of these particle types. In summary, the significant fractions of mineral dust and biological particles in the ice residues suggest their possible favoured role in ice formation.

To further identify the source region of the biological and mineral-dust particles affecting the ice clouds over Wyoming, a global aerosol model, a meteorological model, surface observations, satellite imagery and air mass back trajectory analysis were used. The results, detailed in Supplementary Information, indicate that the dust and biological particles were probably lofted from central China and eastern Mongolia on 29–30 October or 1 November 2007 and transported at an altitude of ~7.5 km across the Pacific Ocean and western United States. These models also show lofting of dust from Sudan or the Sahara[18] occurring on 29–31 October 2007, followed by trans-Asia transport. None of the data supports North America as the source. Supporting the assignment of Asian dust transport, the chemistry of the dust ice residues showed the highest similarity to several Asian dusts and soils in comparison with most North American dusts and soils, discussed further in Supplementary Information. These dust mixing state results demonstrate that it cannot always be assumed that long-range transported dust is always aged, or reacted; this has implications for the treatment of the anthropogenic indirect aerosol effect within mixed-phase cloud models[19], as well as the direct radiative forcing of mineral-dust aerosol within global climate models. Although the long-range co-transport of dust and biological particles at high altitudes has been observed previously[20], long-range transported biological particles have not been directly identified in clouds. Furthermore, the online simultaneous detection of biological and mineral-dust particles suggests a terrestrial source of these biological particles.

Ice-nucleation-active biological particles have been detected previously in precipitation[21]; however, demonstration of a direct connection between biological particles and ice-crystals in clouds has remained elusive[3]. In this study, dual-polarity single-particle mass spectrometry measurements enabled the *in situ* and unambiguous detection of biological particles in cloud ice. This provides the first evidence for the involvement of biological particles, probably bacteria, fungal spores and/or plant material, in ice processes. This was the only ICE-L wave-cloud flight (1 of 9) affected by long-range transported dust, and notably ice-nuclei number concentrations reported herein were among the top 2% of those measured from cloud residues during all ICE-L wave-cloud sampling, supporting the important role that dust and biological particles may have in cloud ice processes. Furthermore, the identification of a significant fraction of biological particles within cloud ice-crystals affected by heterogeneous freezing represents a significant step forward in establishing an understanding of the interaction of biological particles with cloud processes. Herein, long-range transported biological and dust particles involved in cloud ice formation highlight the importance of the interplay between land surface and free troposphere processes and their effects on cloud processes. With increasing frequency and intensity of dust storms predicted as a consequence of climate change and land-use changes in desert regions[1], the presence and transport of biological particles and mineral dust at high altitudes from large-scale dust storms will probably increase and may affect ice-cloud processes, creating previously unidentified climate-system feedbacks and impacts on precipitation, human health and ecosystems.

Methods

A two-dimensional optical array cloud probe (2D-C, Particle Measuring Systems) was used as the primary measurement system for number concentrations of cloud ice-crystals greater than 50 μm in diameter. An extra two-dimensional cloud probe

(2D-S, Stratton Park Engineering Company) measured stereoscopic images for better resolution, compared with the 2D-C, at sizes even below 50 μm. Extra cloud probes used for phase verification are discussed in Supplementary Information. The Wyoming cloud radar and lidar are airborne remote sensors that provided vertical cross-sections from the aircraft to infer properties of cloud particle phase, size and concentration[22,23]. The method of Wang and Sassen[24] using combined aircraft-based lidar and radar measurements was used to derive effective ice-crystal sizes and ice water content as a function of altitude.

Cloud ice-crystals with diameters greater than 7 μm were selected using a CVI; water was evaporated from the crystals at 50 °C, providing residual particles for real-time, *in situ* analysis[7]. Number concentrations of residual particles from 0.5–1.2 μm in diameter were measured using an optical particle counter. To measure the number concentrations of ice-nucleating aerosol particles, a CFDC re-processed ice residues <1.2 μm in diameter (see Supplementary Information) at the cloud observation temperature and at a relative humidity (with respect to water) exceeding 100% (to 103%) to simulate ice formation conditions at expected wave-cloud-parcel entry conditions[8]. The CFDC ice-nuclei data followed Poisson statistics; thus, the standard deviation is noted as the uncertainty. The chemical compositions of individual submicrometre ice residual particles were examined using A-ATOFMS, a recently developed technique that couples aerodynamic sizing and laser desorption/ionization with dual-polarity time-of-flight mass spectrometry[9]. Positive- and negative-ion mass spectra were detected for the time period discussed for 46 cloud ice residues with vacuum aerodynamic diameters from 140 to 700 nm. Standard errors of particle-type number percentages were calculated on the basis of Poisson statistics. Residual particles were classified into distinct types (such as dust versus biological) on the basis of the ion patterns in single-particle mass spectra; peak identifications correspond to the most probable ions for each m/z ratio.

The National Oceanic and Atmospheric Administration Air Resources Laboratory Hybrid Single-Particle Lagrangian Integrated Trajectory model was used for air mass back trajectory analysis[25]. Surface dust simulations were examined using the Navy Aerosol Analysis and Prediction System global aerosol model (www.nrlmry.navy.mil/aerosol/). The Navy Operational Global Atmospheric Prediction System provided weather modelling and observations. Satellite imagery was provided by the National Aeronautics and Space Administration Sea-viewing Wide Field-of-view Sensor (http://oceancolor.gsfc.nasa.gov/SeaWiFS/).

Received 11 December 2008; accepted 16 April 2009; published online 17 May 2009

References

1. IPCC *Climate Change 2007: The Physical Science Basis* (eds Solomon S. *et al.*) (Cambridge Univ. Press, 2007).
2. Lohmann, U. & Feichter, J. Global indirect aerosol effects: A review. *Atmos. Chem. Phys.* **5**, 715–737 (2005).
3. Möhler, O., DeMott, P. J., Vali, G. & Levin, Z. Microbiology and atmospheric processes: The role of biological particles in cloud physics. *Biogeosciences* **4**, 1059–1071 (2007).
4. Jayaweera, K. & Flanagan, P. Investigations on biogenic ice nuclei in the Arctic atmosphere. *Geophys. Res. Lett.* **9**, 94–97 (1982).
5. Saxena, V. K. Evidence of the biogenic nuclei involvement in Antarctic coastal clouds. *J. Phys. Chem.* **87**, 4130–4134 (1983).
6. Deguillaume, L. *et al.* Microbiology and atmospheric processes: Chemical interaction of primary biological aerosols. *Biogeosciences* **5**, 1073–1084 (2008).
7. Ogren, J. A., Heintzenberg, J. & Charlson, R. J. *In-situ* sampling of clouds with a droplet to aerosol converter. *Geophys. Res. Lett.* **12**, 121–124 (1985).
8. Rogers, D. C., DeMott, P. J., Kreidenweis, S. M. & Chen, Y. A continuous-flow diffusion chamber for airborne measurements of ice nuclei. *J. Atmos. Oceanic Technol.* **18**, 725–741 (2001).
9. Pratt, K. A. *et al.* Development and characterization of an aircraft aerosol time-of-flight mass spectrometer. *Anal. Chem.* **81**, 1792–1800 (2009).
10. Baker, M. B. Cloud microphysics and climate. *Science* **276**, 1072–1078 (1997).
11. Fergenson, D. P. *et al.* Reagentless detection and classification of individual bioaerosol particles in seconds. *Anal. Chem.* **76**, 373–378 (2004).
12. Russell, S. C. Microorganism characterization by single particle mass spectrometry. *Mass Spectrom. Rev.* **28**, 376–387 (2009).
13. Richardson, M. S. *et al.* Measurements of heterogeneous ice nuclei in the western United States in springtime and their relation to aerosol characteristics. *J. Geophys. Res.* **112**, D02209 (2007).
14. Cziczo, D. J., Murphy, D. M., Hudson, P. K. & Thomson, D. S. Single particle measurements of the chemical composition of cirrus ice residue during CRYSTAL-FACE. *J. Geophys. Res.* **109**, D04201 (2004).
15. Gallavardin, S., Lohmann, U. & Cziczo, D. Analysis and differentiation of mineral dust by single particle laser mass spectrometry. *Int. J. Mass Spectrom.* **274**, 56–63 (2008).
16. Salam, A. *et al.* Ice nucleation studies of mineral dust particles with a new continuous flow diffusion chamber. *Aerosol Sci. Technol.* **40**, 134–143 (2006).
17. Gallavardin, S. J. *et al.* Single particle laser mass spectrometry applied to differential ice nucleation experiments at the AIDA chamber. *Aerosol Sci. Technol.* **42**, 773–791 (2008).
18. McKendry, I. G. *et al.* Trans-Pacific transport of Saharan dust to western North America: A case study. *J. Geophys. Res.* **112**, D01103 (2007).
19. Hoose, C., Lohmann, U., Erdin, R. & Tegen, I. The global influence of dust mineralogical composition on heterogeneous ice nucleation in mixed-phase clouds. *Environ. Res. Lett.* **3**, 025003 (2008).
20. Kellogg, C. A. & Griffin, D. W. Aerobiology and the global transport of desert dust. *Trends Ecol. Evol.* **21**, 638–644 (2006).
21. Christner, B. C. *et al.* Geographic, seasonal, and precipitation chemistry influence on the abundance and activity of biological ice nucleators in rain and snow. *Proc. Natl Acad. Sci. USA* **105**, 18854–18859 (2008).
22. Wang, Z. *et al. International Conference on Cloud Physics and Precipitation* (Cancun, 2008).
23. Leon, D., Vali, G. & Lothon, M. Dual-doppler analysis in a single plane from an airborne platform. *J. Atmos. Oceanic Technol.* **23**, 3–22 (2006).
24. Wang, Z. & Sassen, K. Cirrus cloud microphysical property retrieval using lidar and radar measurements. Part I. Algorithm description and comparison with *in situ* data. *J. Appl. Meteorol.* **41**, 218–229 (2002).
25. Draxler, R. R. & Rolph, G. D. *HYSPLIT (HYbrid Single-Particle Lagrangian Integrated Trajectory) Model access via NOAA ARL READY Website* (NOAA Air Resources Laboratory, 2003); available at <http://www.arl.noaa.gov/ready/hysplit4.html>.

Acknowledgements

NSF and NCAR are acknowledged for financial support of ICE-L, as well as of A.J.H. K.A. Prather and K.A. Pratt acknowledge NSF for support of ICE-L (ATM-0650659), A-ATOFMS development (ATM-0321362) and a graduate research fellowship for K.A. Pratt. P.J.D. and A.J.P., J.R.F. and Z.W., and C.H.T. acknowledges support from NSF (ATM-0611936, ATM-0645644, and ATM-0612605, respectively). The Office of Naval Research (PE-0602435N) is acknowledged for financial support for D.L.W. Cloud probe data were provided by NCAR/EOL under sponsorship of NSF (http://data.eol.ucar.edu). S. Haimov (Univ. Wyoming) processed the radar data. T. Eidhammer (NCAR) assisted with CFDC data analysis. C. Gaston (UCSD) assisted with the *P. syringae* A-ATOFMS data collection; J. Dixon and R. Dowen III (UCSD) provided the *P. syringae* cultures. S. Kreidenweis (Colorado State Univ.) is thanked for discussions. The authors acknowledge the NOAA ARL for the provision of HYSPLIT (http://www.arl.noaa.gov/ready.html).

Author contributions

K.A. Pratt carried out the A-ATOFMS measurements, data analysis and wrote the manuscript. P.J.D. was responsible for the CFDC measurements and contributed to writing. J.R.F. and Z.W. provided lidar and radar data. D.L.W. carried out the surface and long-range transport modelling. A.J.H. processed the cloud probe data. C.H.T. coordinated and ran the CVI during flight. A.J.P. and K.A. Prather are extra Principal Investigators of this work. All authors reviewed and commented on the paper.

Additional information

Supplementary information accompanies this paper on www.nature.com/naturegeoscience. Reprints and permissions information is available online at http://npg.nature.com/reprintsandpermissions. Correspondence and requests for materials should be addressed to P.J.D. or K.A.P.